Compost: Potent biosorbent for the removal of heavy metals from industrial and landfill stormwater

Pennanen Toni, Srivastava Varsha, Sillanpää Mika, Sainio Tuomo

DOI: 10.1016/j.jclepro.2020.122736

Compost: Potent biosorbent for the removal of heavy metals from industrial and landfill stormwater.

Toni Pennanen*[a], Varsha Srivastava[a], Mika Sillanpää[b,c,d,e], Tuomo Sainio[a]

[a] *Department of Separation Science, Lappeenranta–Lahti University of Technology LUT, Sammonkatu 12, FI-50130 Mikkeli, Finland*

[b] *Institute of Research and Development, Duy Tan University, Da Nang 550000, Vietnam*

[c] *Faculty of Environment and Chemical Engineering, Duy Tan University, Da Nang 550000, Vietnam*

[d] *School of Civil Engineering and Surveying, Faculty of Health, Engineering and Sciences, University of Southern Queensland, West Street, Toowoomba, 4350QLD, Australia*

[e] *Department of Chemical Engineering, School of Mining, Metallurgy and Chemical Engineering, University of Johannesburg, P. O. Box 17011, Doornfontein2028, South Africa*

*__Corresponding Author:__ (email: *Toni.Pennanen@lut.fi*)

Abstract

Stormwater can be contaminated with heavy metals and low-cost solutions are needed to treat large amounts of water. This study was conducted to determine the viability of compost as an adsorbent in Nordic conditions to treat stormwaters. Metal ions chosen for this study were Cadmium(II), Copper(II), Nickel(II), Lead(II) and Zinc(II) and the observed order of adsorption affinities to compost is Lead(II)>Cadmium(II)>Copper(II)>Zinc(II)>Nickel(II). Surface area of compost was determined to be 2.14 m^2/g. Removal of metal ions can be attributed to the compost surface chemical properties due to the –hydroxyl and carboxylic acid functional groups, confirmed by infrared spectroscopy. The zero-point charge of the compost was determined to be 6.53, which favours the adsorption of metal ions at neutral pH. Adsorption is kinetically fast, and it takes less than 10 minutes to reach equilibrium. Equilibrium data were analysed and Cadmium fits with Langmuir, Copper with linear and Nickel, Lead and Zinc with Fowler-Guggenheim isotherm. Thermodynamic study demonstrated the spontaneity of adsorption. The adsorption study at different pH levels revealed that compost neutralises the solution during adsorption, so no further pH adjustment for treated stormwater is needed, and treated stormwater can be directly released into the water stream. The efficiency of the compost was also investigated for real stormwater, and it was found that compost adsorbent is very efficient for the removal of trace concentrations of metallic ions from real stormwater. Lower temperatures do not affect the adsorption process, so compost would be a great choice as low-cost adsorbent material for lower outdoor temperatures, especially in Nordic regions.

Keywords: Stormwater, adsorption, compost, heavy metal

Highlights:

- Adsorption of heavy metals from real and simulated stormwater on compost was investigated.
- Compost neutralises the metal solutions during adsorption.
- Equilibrium is reached within 10 minutes.
- Adsorption process is exothermic, but the values are relatively small except for Cd.
- The performance of compost is therefore expected to improve in cold climate.

1. Introduction

The treatment of stormwaters is a growing trend as environmental awareness increase. In Finland the law dictates the basic lines for stormwater treatment. (1) Planning of the control of stormwaters, (2) Adsorption and delay at its origin, (3) Prevention of damage to environment and property acknowledging the changing climate, and (4). Movement towards dispensing with the feeding of stormwaters to wastewater sewers (*Land use and construction act, 5.2.1999/132, 103 b §*, n.d.). As stormwaters usually contain low concentrations of pollutants compared to traditional wastewaters, directing them to municipal wastewater systems increases water loads and the cost of purification.

The pollutants and their concentration in stormwater are highly dependent on the location where they are created. At least 123 different compounds have been detected in stormwater samples (Fairbairn et al., 2018). Commonly found contaminants in stormwaters are cadmium (Cd), copper (Cu), chromium (Cr), iron (Fe), nickel (Ni), lead (Pb), zinc (Zn), oils, contaminants of emerging concern (CECs), and nutrients (Milik and Pasela, 2018). These contaminants come from wearing car parts, exhaust fumes, rooftops, piping, and lawns (Makepeace et al., 1995). Industrial areas and landfills are locations where special care needs to be taken due to many possible contaminants and higher concentrations. Paved areas at these sites have drains that are not usually connected to the municipal drain system. Industrial areas also have higher heavy metal content and lower chemical oxygen demand (COD) than other stormwaters (Cramer et al., 2019). Heavy metals can have an adverse effect on life as they are toxic, carcinogenic, and bio-accumulative (Fu and Wang, 2011). Cu and Zn are essential for human biochemical processes, but they are needed only in very low concentrations. Excessively high concentrations of these metals can cause symptoms like cramps, vomiting, and irritation. Cd and Ni are carcinogens and

Pb is a neurotoxin (Järup, 2003). When combined all these contaminants pose even greater threat to health and environment (Ye et al., 2017).

Traditionally stormwaters are treated with constructed stormwater ponds, wetlands, bioretention, sand filtration, and enhanced media filtration (Moore et al., 2017). Sedimentation, ponds, and wetlands require large areas to function so they are not usually suitable for urban areas (Reddy et al., 2014). Required land area can be significantly decreased with adsorption methods. Adsorption based methods do not require the addition of chemicals to the water which usually leads to additional steps in other available treatment processes. Adsorption method is rather effective in the removal of trace amounts of metal concentrations. Novel adsorption materials, like graphene, can be efficient in metal removal but possess also multiple problems like cost and environmental friendliness (Liu et al., 2019). Application of low-cost materials can reduce the overall cost of the treatment process (Gusain et al., 2014). Adsorbents/biosorbents that have been tested for stormwater include biochar, ash, sand, iron enhanced sand, zeolite, wood chips, and compost (Seelsaen et al., 2006). Efficiency, selectivity, cost of manufacturing and availability can be a limiting factor for biosorbent use. Composted municipal organic waste is a cheap and renewable source of material. Compost is an organic material created when organic matter decomposes aerobically (Grimes et al., 2002). It has been traditionally used as a soil improver and fertiliser (Milojković et al., 2016). Humic substances and organic soil matter have been shown in previous research to be capable of binding heavy metals (Beckwith, 1959). Compost has also been a good sorbent for other contaminants such as oils and E.coli (Faucette et al., 2009). Combining compost with other adsorbents like biochar could improve overall effectiveness (Tian et al., 2014) and bacteria and fungi in compost can also improve metal

removal (Ye et al., 2019). The previous research of compost has mostly been for bioretention areas and focused to one or two contaminants at a time.

This study is a part of larger project where circular economy solutions are being developed to purify stormwater at the local landfill. In the present study, compost was selected for the treatment of simulated stormwater and real stormwater samples by the adsorption technique. Focus was kept on metal content of the stormwater as oil and dissolved organic carbon content were not a concern. Compost was selected for the study due to its availability, low price, and to deepen the knowledge of its properties and behaviour. Furthermore, it is readily available to use at the local landfill. The detailed textural properties of compost were investigated to understand the mechanism of compost-metal interaction. The effects of different parameters such as contact time, pH, adsorbent dose, and temperature were studied for the optimisation of the adsorption process. Isotherm, kinetic, and thermodynamic studies were conducted to understand the mechanism of adsorbent-adsorbate interaction.

2. Materials and methods

2.1. Adsorbent

Compost used in metal adsorption experiments was collected from a local landfill (Mikkeli, Finland) consisted mostly of municipal garden waste (branches, leaves, grass, vegetables and fruits) and had been composted for two years. The same composted material is usually mixed with sand and sold as commercial garden soil. The composition of compost can change depending on decomposing material but for local use the feed material and conditions stays mainly the same, hence there won't be any significant changes in compost. However, compost was collected twice from two different place for confirmation of its composition and it was observed that there were not significant changes. All larger stones and non-organic objects were

removed before drying and hygienised at 65 °C for 24 h. The dried compost was then ground using tube mill (C S000, IKA, Germany) and sieved , (VWR, ISO 3310-1, 150 µm). The same particle size was used for the whole study. Metal leaching from compost was investigated at different pH values. For this purpose, 0.25 g of compost was added to 50 ml of pH-adjusted water for 24 h contact time. The adsorbent was filtered after 24 h and the metal concentration in the filtrate was measured using an inductively coupled plasma optical emission spectrometer (ICP-OES, iCAP 6300 series, Thermo Fisher Scientific, USA.)

Functional groups of compost were detected using a Fourier transformation infrared spectrometer (FTIR, Bruker Vertex 70, Germany). Surface area was determined by the Brunauer-Emmett-Teller (BET, Tristar II plus, Micromeritics, USA). Physical surface properties were investigated using a transmission electron microscope (TEM, Hitachi H-7700, Japan) and energy-dispersive scanning electron microscope (SEM-EDS, Hitachi S-4800, Japan). Elemental analysis was conducted by means of X-ray photoelectron spectroscopy (XPS, ESCALAB 250, 1486.6 eV Al-K x-ray source, Thermo Fisher Scientific, USA) . The X-ray diffraction pattern for the compost was collected with an X-ray diffractometer XRD, PANanalytical Empyrean series 2, UK, Cobalt anode, λ=1.78 Å, to analyse the composition. The diffraction pattern for compost was collected from 10-100° by maintaining 40 kV voltage and 30 mA current.

2.2. Solutions

Metals Cd, Cu, Ni, Pb, and Zn with oxidation state II, were selected for study as these metals are commonly available in stormwater. Metal solutions for single-solute and multi-solute were prepared using cadmium chloride ($CdCl_2$), copper chloride ($CuCl_2$), nickel chloride ($NiCl_2 \cdot 6 H_2O$), zinc chloride ($ZnCl_2$), and lead nitrate ($Pb(NO_3)_2$). Lead nitrate was chosen over chloride because of its solubility in water. pH adjustments were made using 0.1 M hydrochloric acid

(HCl) and 0.1 M sodium hydroxide (NaOH). The pH of working solutions was between 5.5 and 6. All chemicals were obtained from Sigma-Aldrich (Merck) with purity of 99.99 % trace metals basis.

2.3. Adsorption tests

For metal adsorption experiments, 150 mg of dried compost was measured in a 15 ml tube. 10 ml of metal solution was added in all cases and then kept for shaking at 270 rpm (KS 4000 ic control, IKA, Germany). After shaking for the required time, the solution was filtered using 0.45 µm syringe filters. pH after adsorption was neutral. Metal concentrations before and after adsorption were measured with ICP-OES. Experiments were done twice. The amount of metal adsorbed was calculated using the following Eq.(1):

$$q_e = \frac{(C_i - C_e)V}{m} \quad (1)$$

where q_e is mg of metal adsorbed per gram of adsorbent, C_i and C_e are the initial and final concentrations of metal ions (mg/L), V is the volume (L) of the solution, and m is the mass (g) of the sorbent. The percentage of removal was calculated using the Eq. (2):

$$R\ \% = \frac{C_i - C_e}{C_i} * 100 \quad (2)$$

The adsorption efficiency of compost was investigated for the metal adsorption in single- and multi-solute systems to decipher the trend of metal adsorption in single- and multi-metal solutions. A preliminary test was also carried out with commercial biochar to compare its efficiency with compost as it is also low-cost adsorbent (Inyang et al., 2016). Adsorption kinetics were determined using 150 mg of adsorbent in 10 ml of solution (10-100 mg/l) with different contact times from 1-60 min at room temperature, 23 °C (296 K).

For the adsorption isotherms study, adsorption experiments were conducted with metal solutions of different concentrations (10-200 mg/l) at different temperatures: 5 °C, 15 °C and 40 °C. Lower temperatures were selected to simulate the normal Finnish temperature range. A dose of 150 mg was added to the 10 ml of metal solution and mixed (270 rpm) for one hour. Isotherm data was validated by applying the Linear, Freundlich, Langmuir, and Fowler-Guggenheim isotherm models. Only Linear model is presented as linear, others as non-linear.

Linear isotherm: Eq. (3)

$$Q_e = k * Ce \quad (3)$$

where Q_e = equilibrium uptake in solid phase (mg/g), k = equilibrium constant of adsorption reaction (L/g), and C_e = equilibrium concentration in liquid phase (mg/l)

Freundlich isotherm: Eq. (4)

$$Q_e = K_f \left(\frac{C_e}{C^\circ}\right)^{1/n} \quad (4)$$

where K_f (mg/g) and n (-) are Freundlich constants and C° = 1 mg/L makes the base dimensionless.

Langmuir isotherm: Eq. (5)

$$Q_e = \frac{Q_m b C_e}{1 + b C_e} \quad (5)$$

where Q_m = maximum adsorption capacity (mg/g), b = equilibrium constant of adsorption reaction (L/mg)

Fowler-Guggenheim isotherm: Eq. (6)

$$bC_e = \frac{\theta}{1-\theta} exp(-c\theta) \quad (6)$$

where c = interaction parameter and θ = fractional coverage of adsorption sites is calculated as the ratio of loading and the maximum adsorption capacity (Q_e/Q_m).

Thermodynamic parameters such as change in Gibbs free energy (ΔG^0), enthalpy (ΔH^0), and entropy (ΔS^0) were taken into consideration to determine the spontaneity and other aspects of a given adsorption process. Change in Gibbs energy can be calculated using the Gibbs-Helmholtz equation (Bulut and Aydin, 2006). Eq. (7) and Eq. (8)

$$\Delta G^o = -RTln\,(b * M * 1000 * C^0) \quad (7)$$

$$\ln b = \frac{\Delta S^o}{R} - \frac{\Delta H^o}{RT} \quad (8)$$

where ΔG^o = change in Gibbs free energy (J/mol), R = gas constant (8.314 J/mol K), T = temperature (K), ΔH^o = change in enthalpy (J/mol) and ΔS^o = change in entropy (J/molK). Because the unit of parameter b is L/mg, the argument of the logarithm function in Eq.8 needs a multiplier 1000*M*C^0 where M = molar mass of metal and C^0 is unit concentration (mol/L). In case of linear isotherm, the factor 1000 is omitted.

After optimisation of the adsorption process parameters, the adsorption experiment was conducted with two different real stormwater samples in optimum conditions. The pH of the real stormwater samples was 7.5 and adsorption experiments were conducted without changing the pH of the stormwater to demonstrate the adsorption efficiency of the compost.

2.4. pH_{zpc} and effect of pH

To determine the zero-point charge (pH_{zpc}), 0.25 g of compost adsorbent was added to 50 ml of pH-adjusted (2-12) ultrapure water and kept in contact for 48 h at room temperature (Schwarz et

al., 1984). pH adjustments were made using 0.1 M HCl and 0.1 M NaOH and pH was measured with a pH meter (inoLab pH 730, WTW, USA). The pH was measured after 48 h and a graph was plotted between initial pH and final pH.

The effect of pH on metal adsorption by compost was studied by varying the metal solution pH from 2-12. The pH of the treated solution was also measured to investigate the final pH. For the pH study, the adsorption experiments were conducted over a 1 h contact time using a compost dose of 150 mg with 10 ml of metal solution.

3. Results and discussion

3.1. Characteristics of compost adsorbent

3.1.1. Morphology

To determine compost surface morphology, TEM and SEM analysis was used. It is clear from the SEM image of the compost that its surface is rough with no significant pores detectable (Fig. 1a). The TEM image shows that particles are agglomerated and consist of particles with different diameters (Fig. 1b). The elemental composition of the compost was surveyed with XPS and SEM-EDS and is presented in Table 1. The main components are carbon and oxygen, which is to be expected from an organic compound. The relatively high amounts of iron and silicon can be explained by rocks and sand mixed in the compost. Aluminium and carbon values may have been affected by the aluminium sample tray and carbon tape used to attach samples during SEM analysis.

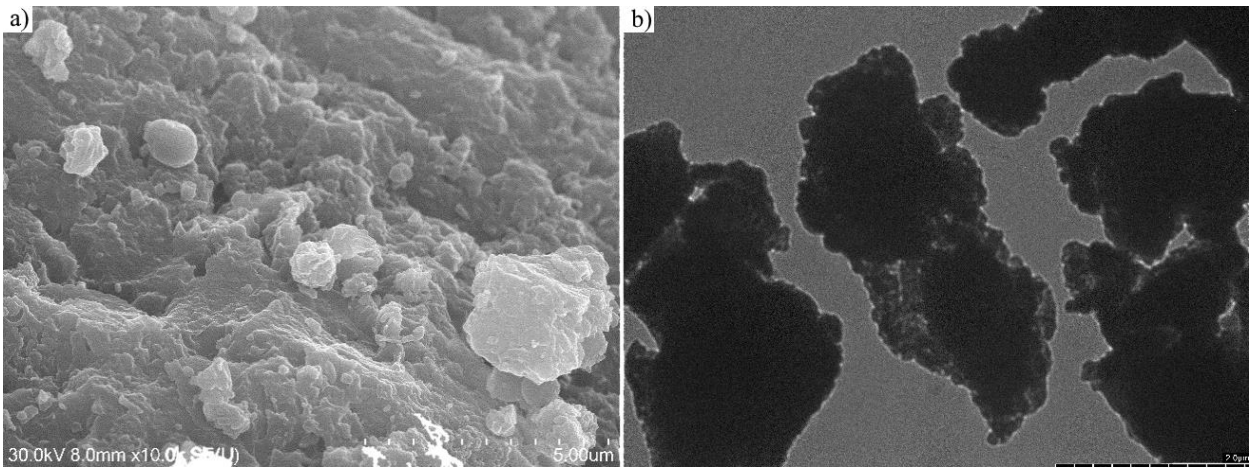

Fig. 1. a) SEM image of compost at 10k magnification b) TEM image of compost at 10k magnification.

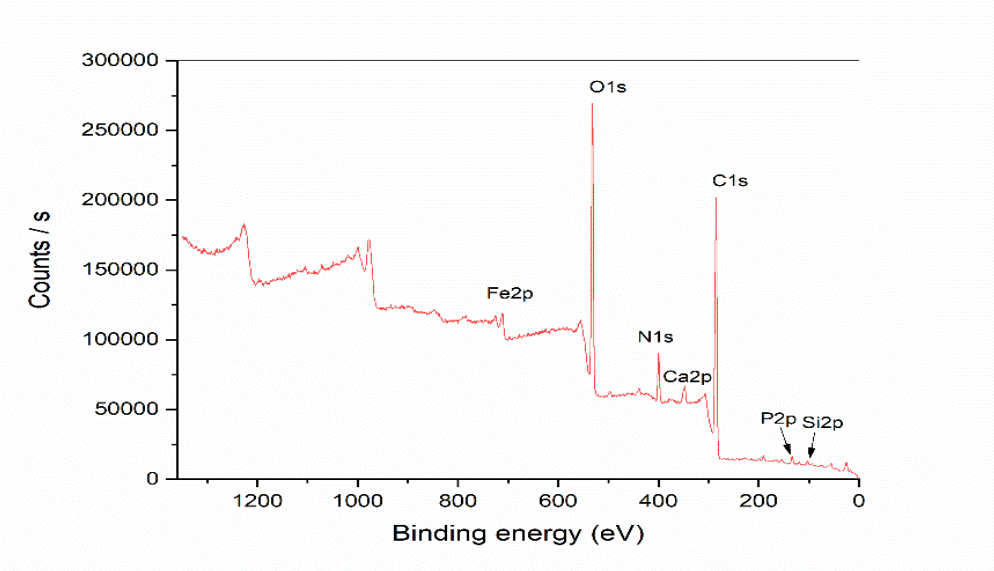

Fig. 2. XPS of bare compost

XPS results (Fig. 2) are in line with EDS. The C 1s area has two peaks C_1 at 284.7 eV which indicates carbon bound to carbon or hydrogen and C_2 at 287.7 eV represents carbon bound to non-carbonyl oxygen (Popescu et al., 2009). The O 1s peak is wide, 530.4-533.3 eV, and can point to groups C=O, Fe-O and C-O (Zhang et al., 2019). The peak of N 1s is at 399.8 eV N connected to -CH. The peak of P 2p is at 133.1 eV and might stem from fertilisers and cells of

organic matter. The peak of Si 2p at 103 eV belongs to SiO_2. The peaks of Fe 2p is at 712.4 eV and 710.8 eV and can be Fe^{2+} or Fe^{3+} (Graat and Somers, 1996) . The peaks of Ca 2p at 347 eV can be CaO or $CaHPO_4$ (National Institute of Standards and Technology. Gaithersburg, 2012).

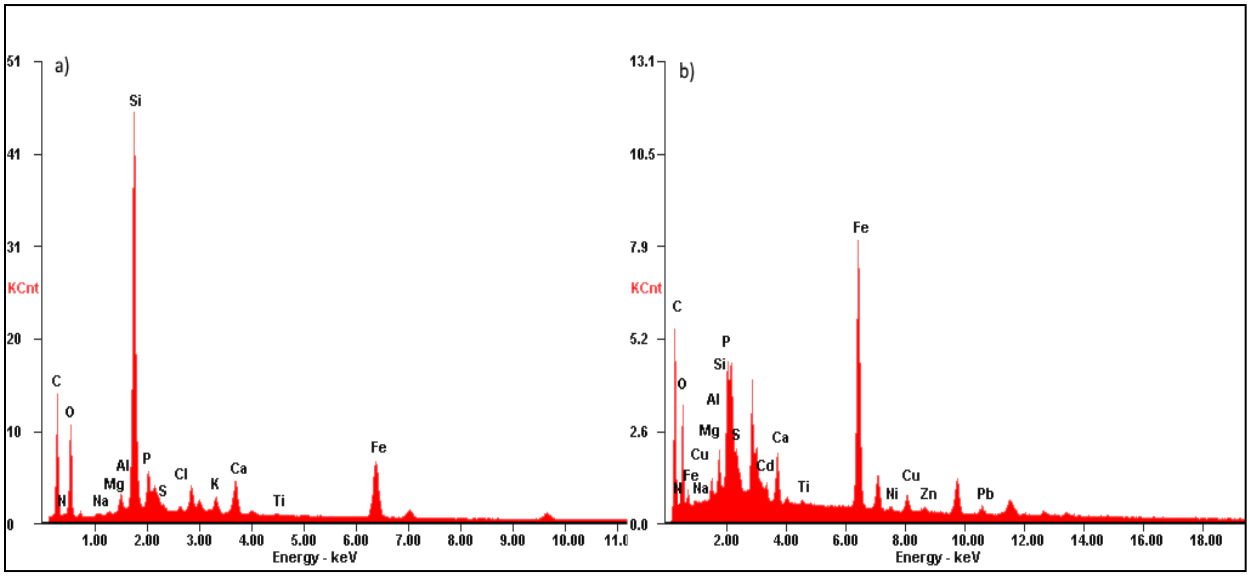

Fig. 3. a) EDS energy diagrams compost before adsorption, and b) EDS after adsorption.

From the SEM-EDS graph (Fig. 3) taken after adsorption it can be seen that the compost contains the removed metal ions.

The XRD pattern has peaks at 24^0, 30.9^0, 58.8^0, and 80.9^0, which correspond well with quartz SiO_2 (ICSD-Ref. 98-000-0174) (Fig. 4) (Degen et al., 2014).

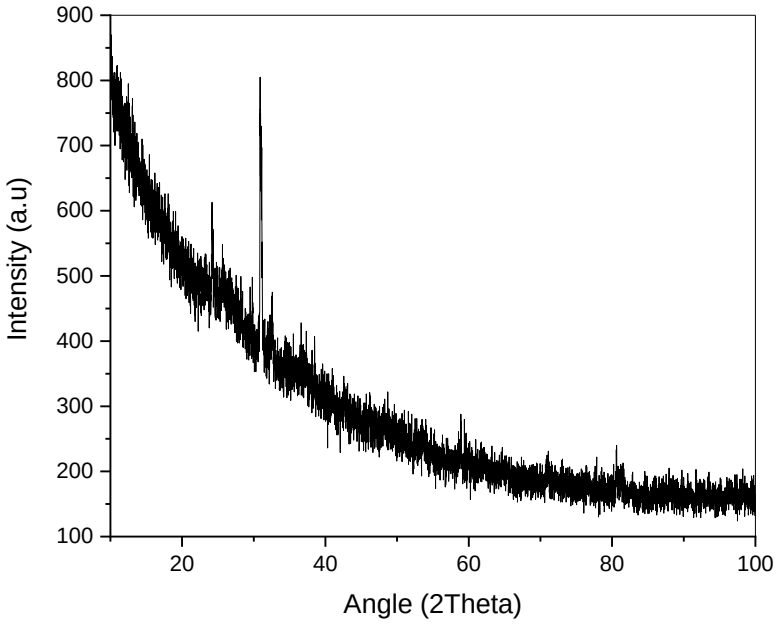

243

244 **Fig. 4.** XRD pattern of bare compost

245 **Table 1.** Elemental composition, by EDS, of compost before and after adsorption (100 mg/l
246 solution).

	Raw	**Cd**	**Cu**	**Ni**	**Zn**	**Pb**	**Multi**
Element	Wt%	Wt%	Wt%	Wt%	Wt%	Wt%	Wt%
C	56.18	46.74	47.22	36.11	51.10	30.99	41.02
N	2.85	8.41	10.94	20.51	8.82	15.67	11.32
O	21.45	19.10	27.71	21.90	22.63	21.88	23.21
Na	0.40	-	0.24	0.06	1.04	0.27	0.17
Mg	0.26	0.21	0.19	-	0.19	-	0.05
Al	1.87	1.06	0.45	0.43	0.67	1.12	0.45
Si	5.93	1.13	0.56	0.85	1.26	7.14	9.31
P	1.69	1.11	1.86	3.91	2.18	3.18	2.36
S	0.47	0.59	0.73	-	0.53	-	0.85
Ca	1.74	4.10	2.41	3.19	2.46	5.33	0.63
Ti	0.13	0.20	0.08	0.09	0.10	0.22	0.09
Fe	5.83	14.37	6.37	10.71	7.18	11.88	7.20

Pb	-	-	-	-	-	2.46	2.46
Ni	-	-	-	2.18	-	-	0.18
Cu	-	-	1.40	-	--	-	0.80
Zn	-	-	-	-	1.77	-	0.31
Cd	-	2.44	-	-	-	-	1.01

As demonstrated by the EDS of the bare sample, sample also has Al, Si, Ti, P, and Fe and these metals can be leached out under highly acidic conditions. The possibility of leaching these metallic ions in acidic and alkaline media was investigated in a metal-leaching experiment and the release of Al, Fe, P, and S was detected. The leaching of metals is greater in acidic or basic solution. Minor leaching was detected at pH 7. For sulphur, leaching is rather stable at all pH values. Metal leaching is presented in Table 2. This study suggests that the compost can be efficiently used for the treatment of stormwater at natural pH. Chemical oxygen demand (COD) however rose after treatment from 0 to 200 mg/l in batch equilibrium tests. This is expected to decrease with time if compost is used in a flow-through system.

Table 2. Metal leaching from compost, compost dose 5 g/l

pH	Al (mg/l)	Fe (mg/l)	P (mg/l)	S (mg/l)
2	3.88	12.92	8.68	3.33
4	0.65	4.19	6.03	3.69
7	0.02	0.38	1.54	3.67
10	1.15	6.74	3.7	5.69

3.1.2. Functional characteristics

Functional groups of compost were examined by FTIR-ATR in the wavelength range 4,000-400 cm^{-1} Table 3. The FTIR spectra of bare compost and metal-adsorbed compost are presented in Fig. 5. The peak observed at 533 cm^{-1} represents iron(II,III) oxide Fe_3O_4 (Vahur et al., 2016). The wide peak at 3,285 cm^{-1} belongs to a typical acid group while the peaks at 2,925 cm^{-1} and 2,852 cm^{-1} can be assigned to CH_2 and CH_3 groups respectively. These peaks correspond with humic acids (SDBS) (Deiana et al., 1990). The strong peak at 1,029 cm^{-1} indicates the presence

of an -OH group., the Peaks of most active functional groups disappear after adsorption and small peaks for $-CH_2$ and $-CH_3$ carbon body and -OH remain. The peaks at 400-500 cm^{-1} are associated with metal binding. -COOH and -OH surface groups were not observed in the FTIR of commercial biochar (Fig. S.1).

Table 3. FTIR spectra of compost

Wavenumber cm^{-1}	**Functional group**
3285	-COOH, -C-H (aromatic)
2925-2852	Aliphatic $-CH_2$, $-CH_3$
1631-1551	Amide,
1410-1389	Aliphatic -C-H
1029	-OH
725-697	Amide, out of plane stretch
533	Iron (II, III) oxide Fe_3O_4

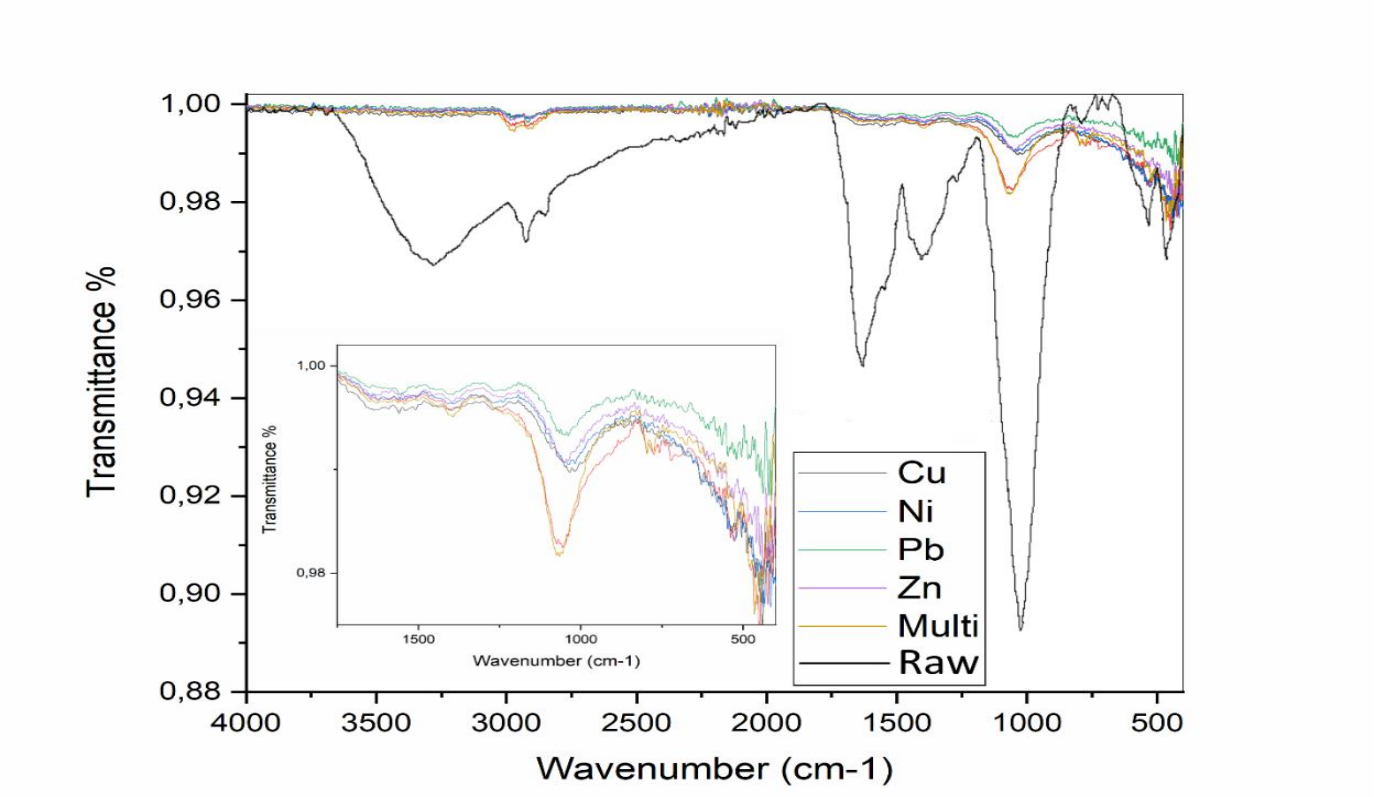

Fig. 5. FTIR spectra of compost before and after adsorption.

3.1.3. BET surface area and porosity

As pore size and surface area contribute greatly to the adsorption process, it is important to determine the porosity and surface area of the adsorbent material. The BET surface area of the compost is very low at 2.14 m^2/g and the pore size is 95.53 Å so compost adsorption properties cannot be attributed to pores and surface area. Commercial biochar has a surface area of 550 m^2/g. These results are in good agreement with SEM where no porous structure was observed for compost. So it can be stated that the compost adsorption efficiency is mainly dependent on the surface chemical properties. The BET surface area plot is presented in Fig. 6a.

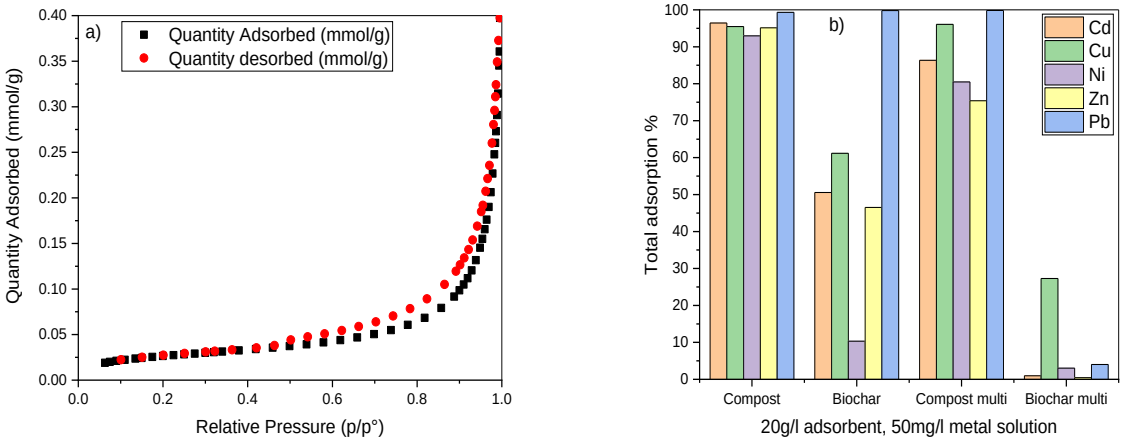

Fig. 6.a) N_2 adsorption−desorption isotherm linear plots (BET) for compost; b) Comparison of the removal efficiency of compost and commercial biochar.

3.2. Adsorption parameters

The adsorption efficiency of compost for the removal of Cd(II), Cu(II), Ni(II), Pb(II), and Zn(II) from single- and multi-solute solution was investigated by varying different parameters. The adsorption efficiency of the compost was also compared with commercial biochar. These experiments showed that with same mass of adsorbent compost can adsorb metal ions more efficiently than commercial biochar (Fig. 6b). With an adsorbent dose of 20 g/l in 50 mg/l of metal solution, compost can remove all the selected metals with over 90% efficiency while biochar does not show very promising results in either a single- or multi-metal solution. However, for Pb ions biochar was found to be equally good as compost. The compost gave better removal for all metal ions in comparison to commercial biochar. The lower removal may be attributable to the absence of some surface groups which are available in compost but not in biochar. Due to the higher efficiency of compost, further study was conducted with compost.

3.2.1. Effect of adsorbent dose on metal adsorption

The effectiveness of compost adsorbent was investigated by changing the adsorbent mass in the range of 5-30 g/l. A different amount of adsorbent was added in 50 mg/l of metal solution and experiments were conducted at room temperature for 1 h of contact time. The results are presented in Fig. 7. Zn and Ni show a lower adsorption percentage than others at small doses. In single-solute solution the adsorption percentage goes from 82.0% to 99.4% (Fig. 7a) while in multi-metal solution decreased adsorption was observed for all metallic ions except Pb (Fig. 7b).

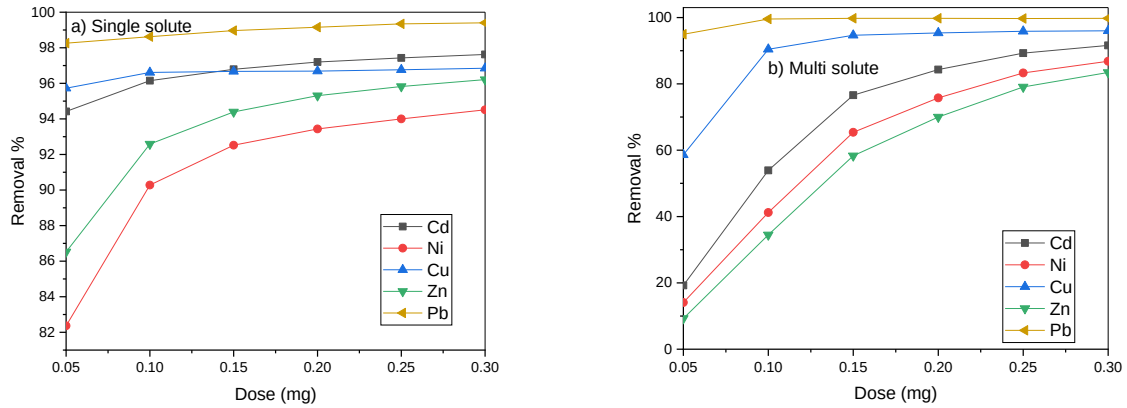

Fig. 7. Effect of dose on metal removal, a) single-solute systems, b) multi-solute system.

Higher removal of metals was observed when a higher dose of compost was used for adsorption. At the higher dose, more active sites are available for the interaction of metal ions, so enhanced removal was recorded at the higher dose, but there is no significant change in removal efficiency (Abu-Danso et al., 2018). For the same amount of adsorbent dose, the removal of metals is lower in multi-metal solution because in a multi-solute system there are more ions present to compete for available sites. At 15 g/l the adsorption process starts to stabilise, and then negligible improvement was recorded in adsorption percentage. That is why a dose of 15 g/l was chosen for the rest of the study.

3.2.2. Effect of contact time on metal adsorption

The equilibrium time is a very important factor in the real-scale applications of any adsorbent material. Metal removal reaches over 90% in one minute in all single-metal solutions (Fig. 8). Adsorption equilibrium seems to be achieved in 10-20 minutes but after that there is no significant increase in the removal percentage of metal ions. In the case of the multi-solute system (Fig. 8) removal percentages are lower as is to be expected when different metals compete. Cd, Ni, and Zn show a sharp decrease in adsorption as concentration rises. Cu and Pb show stable and high equilibrium after 10 minutes.

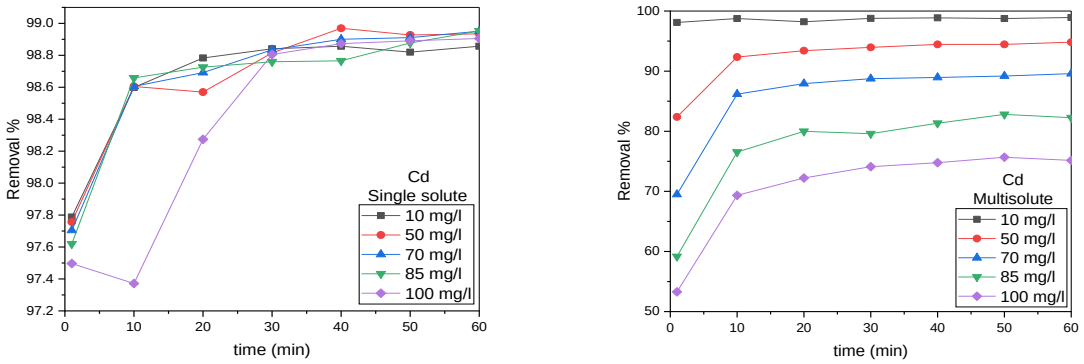

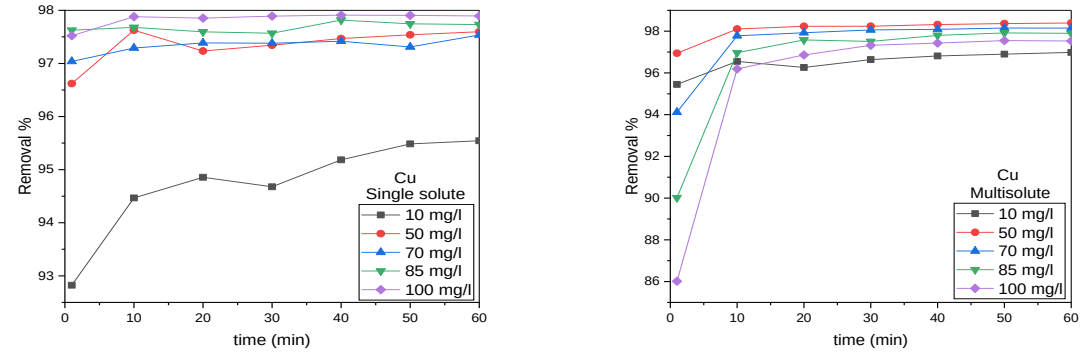

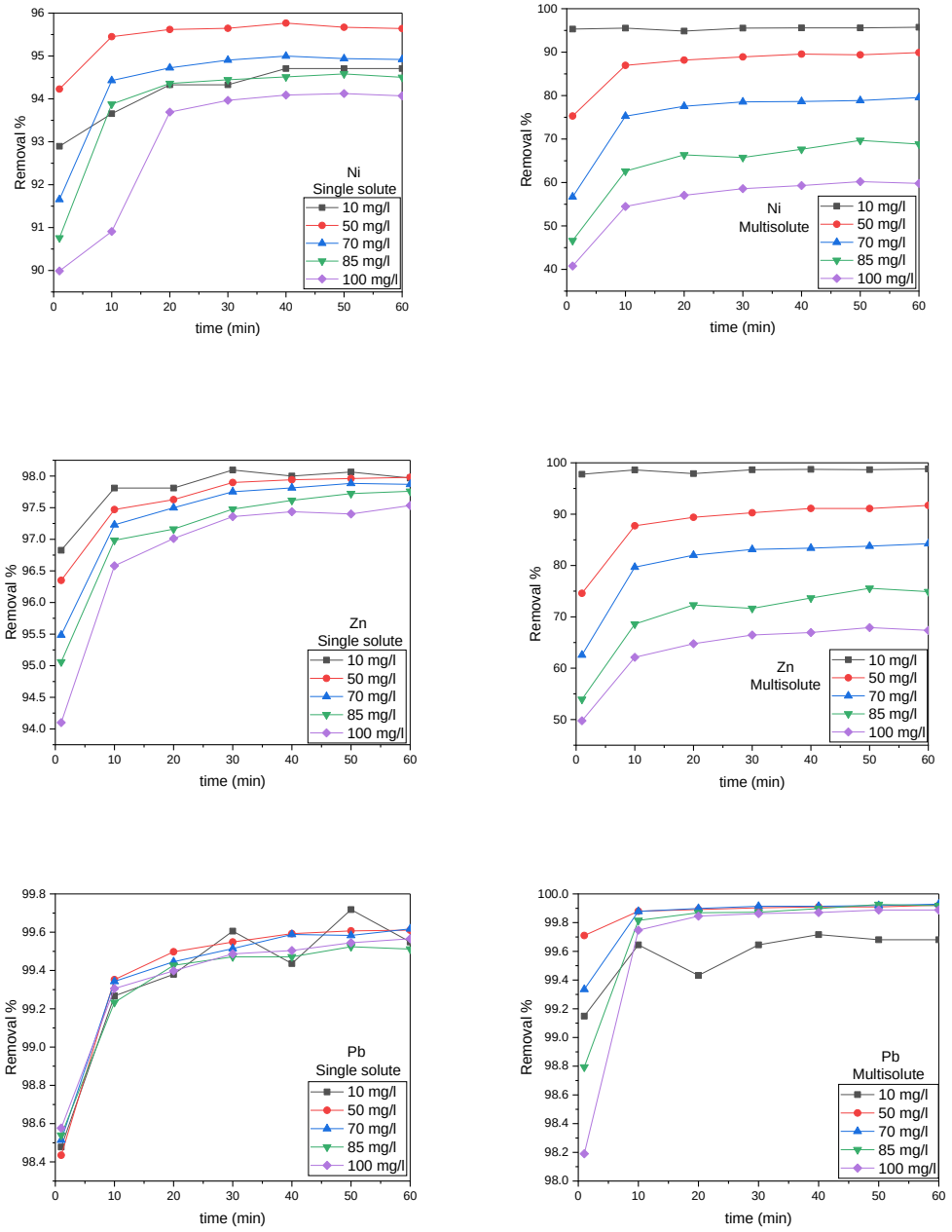

Fig. 8. Effect of contact time on single- and multi-solute systems.

3.2.3. pH_{zpc} of compost and effect of pH on metal removal

The pH of solutions plays an important role in the adsorption of any metallic ions as it can affect the surface nature of the adsorbent. Metals are dissolved at low pH but at high pH they start to

form hydroxides and precipitate. Zn and Cd precipitation start to be effective at pH > 9 (Charerntanyarak, 1999), Cu precipitation at pH > 6 (Albrecht et al., 2011), Ni at pH>10.4 and Pb at pH > 9.6 (Karimi, 2017). The pH_{zpc} of compost was determined to be 6.53 (Fig. 9). If the pH of a solution is < pH_{zpc} then the surface of compost is positively charged while at higher pH(pH > pH_{zpc}) the surface is negatively charged (Hokkanen et al., 2018). At low pH, there are repulsion forces between H^+ and positively charged metal ions and this repulsion can reduce adsorption (Iftekhar et al., 2018). It can be seen from Fig. 10 that adsorption efficiency increases with increasing pH. At higher pH, there is more probability of precipitation, so the experiments were conducted at neutral pH. It was also noticed that, after adsorption, the pH values of treated solutions were neutral which suggests that wastewater treated by compost can be directly released into water streams without any further adjustment step.

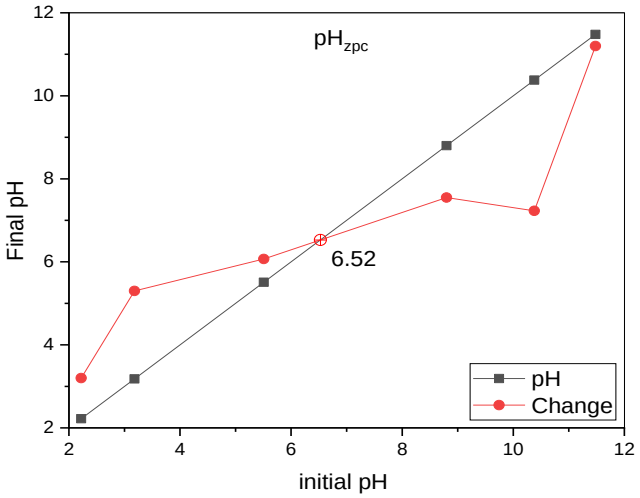

Fig. 9. pH of zero-point charge for compost

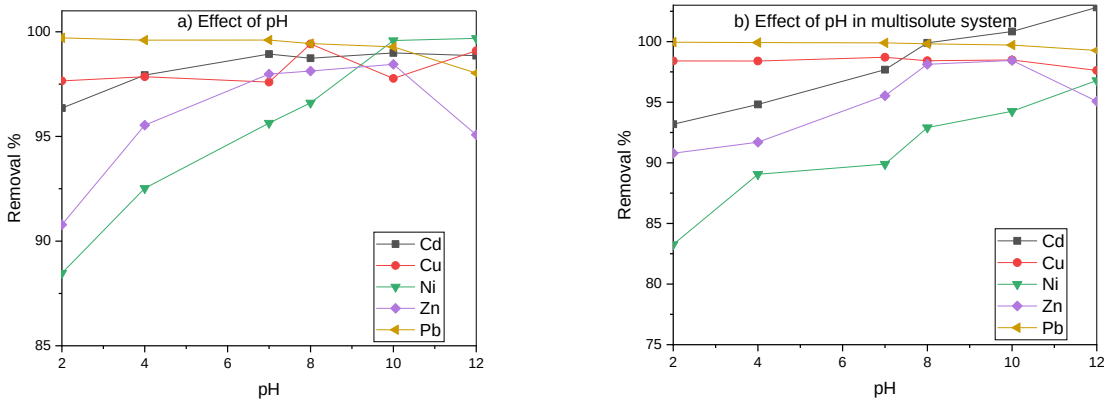

341

342 **Fig. 10.** Effect of pH on metal adsorption a) single-solute, b) multi-solute systems

343 4. Mechanism of metal adsorption on compost adsorbent

344 As shown in Fig. 11, the metal can interact with the compost surface by complex formation or
345 ion exchange. Metal ions can attach to amide groups present in the organic material of compost
346 (McKay et al., 1999). Ions can react with hydroxy and acid groups in the compost. Silicon-,
347 aluminium- and titanium oxide can bind with metal ions in many ways (Naderi Peikam and
348 Jalali, 2019). Ion exchange where calcium is changed to metal also happens. The presence of
349 calcium ions was confirmed by SEM-EDS and XPS analysis.

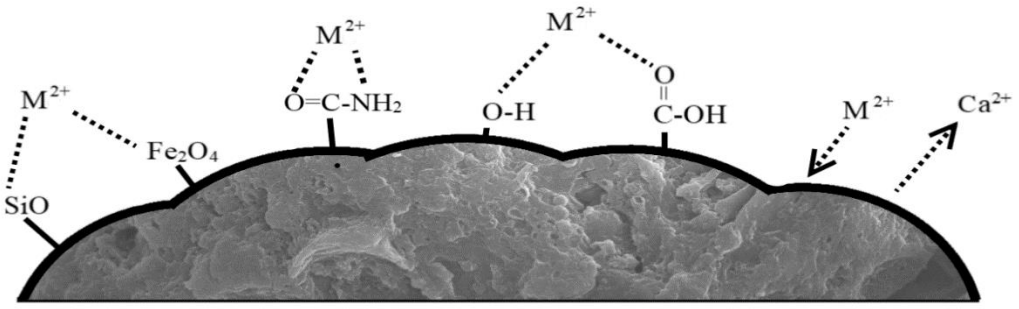

350

351 **Fig. 11.** Possible mechanism of adsorption.

5. Adsorption equilibrium isotherms

Analysis of adsorption equilibrium isotherms, *i.e.* the relationship between adsorbate concentration in the liquid phase and in the solid phase provides further information about the adsorbent and is necessary for assessing the suitability of the adsorbent in practical applications. Adsorption equilibrium data were correlated using the linear, Freundlich, Langmuir, and Fowler-Guggenheim isotherm models. This set of isotherm models can be used to determine whether the surface is heterogeneous or homogeneous for adsorption and if there are significant interactions between adsorbed species.

Adsorption equilibrium data can be correlated with the linear isotherm Eq. (3)(Cantrell et al., 2002). When the adsorbent surface is homogeneous, there are plenty of adsorption sites available and there are no lateral interactions between the adsorbed species (Fig. 12.).

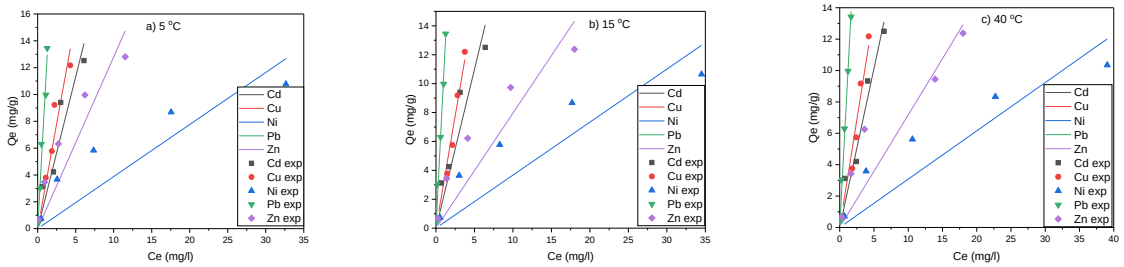

Fig. 12. Linear isotherms a) 5 °C b) 15 °C c) 40 °C

The Freundlich isotherm, non-linear, Eq. (4) is an originally empirical model that describes assumes multiple mono-layer adsorption of any adsorbate species on an energetically heterogenous surface (Freundlich, 1932). The equation can be derived also by assuming that the number of adsorption sites with a given adsorbent-adsorbate interaction energy decreases

exponentially with increasing interaction energy (Do, 1998). The values for each variable are presented in Table 4 and plots in (Fig.13).

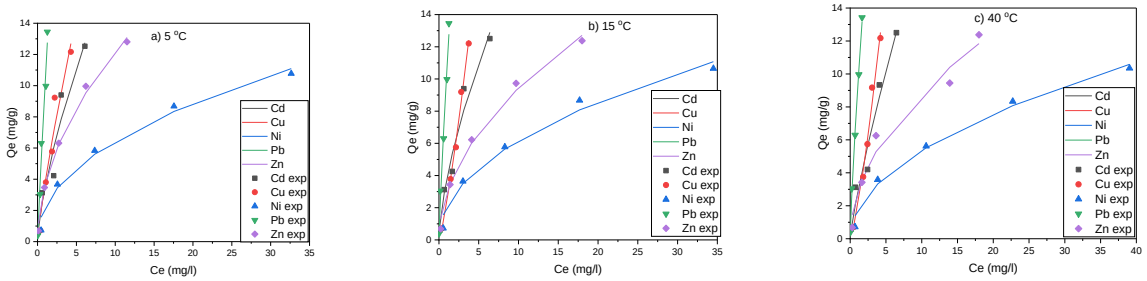

Fig.13. Freundlich isotherms a) 5 °C b) 15 °C c) 40 °C

Langmuir isotherm, Eq. (5), assumes monolayer adsorption on an energetically homogeneous surface where there are no lateral interactions between adsorbed species. Owing to the assumption of a monolayer, the adsorbent has a limited adsorption capacity (saturation capacity) (Chen, 2015). The best-fit parameters for Langmuir isotherm, obtained by non-linear regression, are presented in Table 4 and plots in Fig. 14.

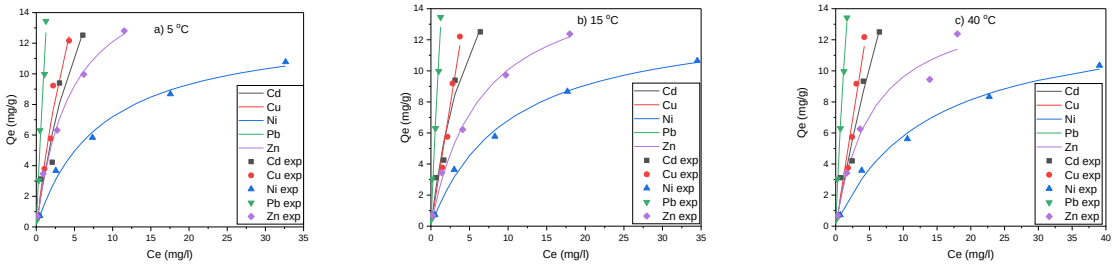

Fig. 14. Langmuir isotherms a) 5 °C b) 15 °C c) 40 °C

Fowler-Guggenheim isotherm, Eq. (6), is one of the simplest models that assume an energetically homogenous surface but there are lateral interactions between adsorbed species (Rangabhashiyam et al., 2014). The interactions can be either attractive or repulsive. If they are attractive, the heat of adsorption increases linearly with surface coverage. When there is no

interaction between species, this equation will reduce to the Langmuir isotherm. The use of this three-parameter isotherm model is slightly more complicated than the two-parameter models discussed above because it is not explicit. An iterative solution is needed to calculate the solid phase concentration at equilibrium as the fractional coverage is present in the exponential term. Best-fit parameters obtained by non-linear regression are presented in Table 4 and plots in Fig. 15.

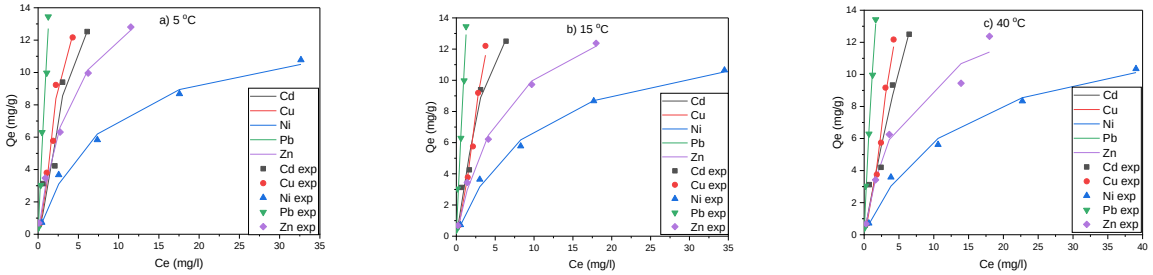

Fig. 15. Fowler-Guggenheim isotherms a) 5 °C b) 15 °C c) 40 °C

Table 4. Estimated parameter values and index of determination (R^2) for adsorption equilibrium isotherms.

		Langmuir parameters			**Freudlich parameters**			**Linear parameters**		**Fowler-Guggenheim**			
	T (K)	Qm mg/g	b	R^2	1/n	k_f	R^2	k	R^2	Q_{max} mg/g	b	c	R^2
Cd	313	57.16	0.044	0.9577	0.82	2.71	0.9622	2.026	0.9492	35.84	0.07	0.63	0.9575
	288	23.96	0.18	0.9715	0.65	3.83	0.9655	2.20	0.8724	16.56	0.18	1.35	0.9740
	278	29.14	0.13	0.9328	0.69	3.62	0.9359	2.26	0.8788	15.48	0.13	2.11	0.9353
Cu	313	2124.13	0.001	0.9539	1.30	1.91	0.9841	2.74	0.9546	17.08	0.10	2.38	0.9867

	288	1591.76	0.002	0.9720	1.26	2.36	0.9934	3.12	0.9728	16.81	0.12	2.34	0.9895
	278	37.83	0.11	0.9490	0.82	3.86	0.9366	3.12	0.9094	14.98	0.15	2.39	0.9713
Ni	313	13.58	0.074	0.9903	0.49	1.70	0.9886	0.31	0.7207	13.58	0.07	3.58 E-06	0.9903
	288	13.56	0.10	0.9936	0.47	2.08	0.9798	0.37	0.6300	13.56	0.10	0.0009	0.9936
	278	13.17	0.12	0.9906	0.46	2.25	0.9841	0.39	0.6289	13.17	0.12	0.001	0.9906
Pb	313	47.86	0.23	0.9900	0.79	8.79	0.9954	8.28	0.9795	46.54	0.23	0.05	0.9899
	288	115.27	0.10	0.9776	0.85	10.58	0.9825	10.52	0.9767	82.27	0.14	0.33	0.9774
	278	94.91	0.12	0.9726	0.91	10.34	0.9732	10.29	0.9703	46.09	0.25	0.66	0.9721
Zn	313	14.81	0.18	0.9705	0.50	2.77	0.9686	0.72	0.7775	14.81	0.18	0.001	0.9705
	288	16.53	0.16	0.9954	0.51	2.94	0.9915	0.79	0.7489	16.52	0.16	0.0007	0.9954
	278	17.57	0.22	0.9939	0.51	3.73	0.9949	1.28	0.7739	17.57	0.22	0.0001	0.9939

Cd adsorption is best explained with Langmuir model. Fowler-Guggenheim model gives same b values but c values are unreasonably large which indicates overfitting with the three-parameter model. Therefore, adsorption can be best explained by simpler model Langmuir model. Cu adsorption correlates equally well with Freundlich and linear models. As the linear model is simpler and does not predict infinite adsorption strength at low concentration it is chosen to describe Cu adsorption. Ni, Pb, and Zn adsorption fit best to the Fowler-Guggenheim model. Inspection of the parameter values shows that this model almost reduces to the Langmuir isotherm in most cases. The values of the c parameter are very small which means there are almost no interactions with the adsorbed species. Limited number of adsorption sites explains the curvature of the isotherm data. If calculation speed is an issue, adsorption of Ni, Pb, and Zn can

406 be almost equally well described with the Langmuir isotherm than with the Fowler-Guggenheim
407 model.

408 The adsorption capacity of compost was also compared to some other biosorbents and it is clear
409 from Table 5 that the efficiency of compost for the selected metallic species is comparable for
410 other adsorbent materials. However, it can be seen that in most of the cases adsorption studies
411 were conducted in an acidic pH range while in the present study reaction parameters were
412 optimised at a natural pH value. The pH of the treated solution was in a neutral range after
413 treatment which make this compost more suitable as no additional pH adjustment step will be
414 needed for treated water before being discharged into the water stream.

415 **Table 5**. Comparison of other biosorbents for biosorption.

Adsorbent	Dose (g/l)	Metal ion	Concentration (mg/l)	pH	Q_{max} Experimental (mg/l)	Efficiency %	Ref.
Compost	40	Cu	20	4.8-7	23.45	92	(Kocasoy and Güvener, 2009)
Compost	40	Zn	10	4.8-7	20	66	
Compost	40	Ni	10	4.8-7	8.75	82	
Peanut shells	20	Cu	150	-		83	(Ali et al., 2016)
Biochar (hardwood)	10	Cu	254	5	6.79	-	(Tan et al., 2015)
	10	Zn	261	5	4.65	-	
lignin	2-6	Pb	20	5	1.38	40	(Srivastava et al., 1994)
Lignin	2-6	Zn	20	5	0.07	53	
Banana peel	30	Cd	30-80	3	5.71	-	(De Gisi et al., 2016)
Banana peel	40	Pb	30-80	5	2.18	-	
Potato peel	10	Cu	150-400	6	0.39	-	
Olive stones	-	Ni	8.8	5.5	2	-	(Fiol et al., 2006)
Compost	15	Cu	100	7	5.78	97.9	In present study
		Cd	100	7	5.22	98.9	
		Ni	100	7	5.96	94.0	
		Pb	100	7	6.31	99.5	
		Zn	100	7	6.34	97.5	

416

5.1. Adsorption kinetics

Adsorption of metals on the compost adsorbent is very fast. Fig. 16 shows that the loading reaches 95% of the equilibrium value within one minute for all other metals and is constant from 10 minutes forward. Since equilibrium is reached this fast, no kinetic modelling can be done based on the data produced with conventional methods.

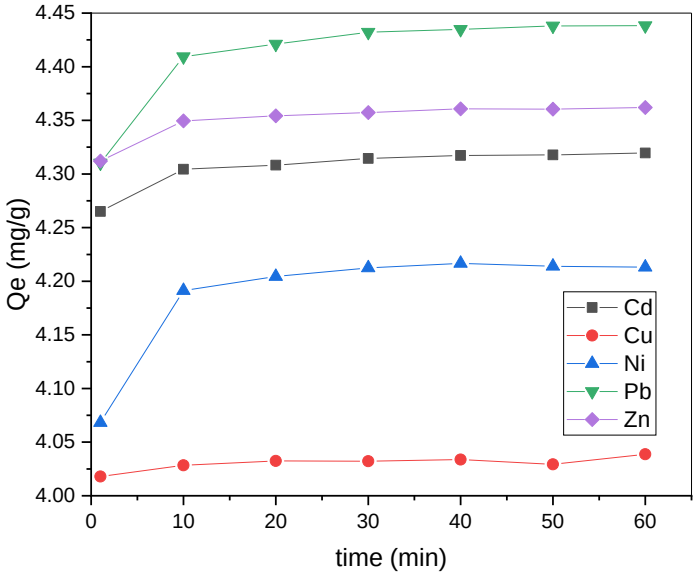

Fig. 16. Loading of metals on the adsorbent as function of time

5.2. Effect of temperature and thermodynamic study

Temperature can affect the adsorption of any pollutant species as temperature variation affects the mobility of ions, adsorbent surface pore enlargement, etc. For the investigation of temperature effect solution temperature was varied from 278 to 313 K. However, no significant effect on the adsorption capacity of the compost was observed when temperature was varied from 278-313 K.

Thermodynamic parameters ΔH^o and ΔS^o were obtained using Eq. (7) and (8). Linear isotherm was used for Cu and Pb whereas Langmuir isotherm was used for the others. Thermodynamic parameters are presented in Table **6.** Thermodynamic parameters for the adsorption of metal ions on compost adsorbent6. Negative values of ΔG^o suggested that reaction is spontaneous. ΔG^o values range from -19 to -25 kJ/mol for all metals indicating that adsorption on compost is not irreversible. Negative ΔH^o indicates that the adsorption process is exothermic, but the values are relatively small except for Cd. The performance of compost is therefore expected to improve in cold climate. Values of ΔS^o are positive but small indicating that adsorption is enthalpy-driven because disorder increases in the system.

Table 6. Thermodynamic parameters for the adsorption of metal ions on compost adsorbent

Metal ions	ΔG^o 315.15K (kJ/mol)	ΔG^o 288.15K (kJ/mol)	ΔG^o 278.15K (kJ/mol)	ΔH^o (kJ/mol)	ΔS^o (J/mol K)
Cd	-22.27	-23.70	-22.11	-24.17	-5.02
Cu	-21.81	-20.24	-19.55	-2.74	60.57
Ni	-22.02	-20.85	-20.54	-9.25	40.45
Pb	-24.70	-23.16	-22.30	-4.75	63.45
Zn	-24.63	-22.11	-22.15	-3.54	66.91

5.4. Investigation of the adsorption efficiency of compost adsorbent for a real stormwater sample

Two samples of real stormwater were tested for metal content and an adsorption study was conducted in optimised conditions. The concentration of metal ions was very low in real stormwater collected from Mikkeli, Finland. Samples were taken at different times from the same location as metal concentration may vary at different times of a season. It was observed that samples collected at different time have different concentrations and compositions. Both samples had pH ~ 6.5. The samples show small concentrations of metallic pollutants Table 7.

The compost was found to be very efficient in the removal of metallic ions from stormwater where the concentrations of metallic ions were very low although aluminium seems to be unaffected. Higher concentrations of Ca and Na are due to the leaching of these ions from the compost.

Table 7. ICP-OES results for real stormwater samples.

Stormwater sample	Al (μg/l)	Ca (mg/l)	Cu (μg/l)	Fe (μg/l)	Zn (μg/l)	Na (mg/l)	Ni (μg/l)
Stormwater (W1) before treatment	40	16	20	70	120	0.99	10
Stormwater (W1) after treatment	40	38	10	5	20	28.6	0
Stormwater (W2) before treatment	0	26	10	20	80	1.8	0
Stormwater (W2) after treatment	0	50	0	4	20	28.3	0

6. Conclusions

A low-cost compost material was used as an adsorbent for the removal of Cd(II), Cu(II), Ni(II), Zn(II), and Pb(II) from simulated stormwater and real stormwater samples. The dosage of adsorbent plays a significant role in metal adsorption. Adsorption equilibrium was achieved in less than one hour. Increasing the pH of solutions increases the metal ion removal percentage but after pH moved to the alkaline range the removal was due to precipitation. Further, after treatment pH of the treated solution was in the neutral range for all metals, which suggests that there is no need to apply additional treatment to pH adjustment before release into the water stream. Experiments were also performed without acidification. An FTIR study showed that –OH and –COOH functional groups play significant roles in the metal removal process. A thermodynamics study demonstrated that metal adsorption on compost is spontaneous.

Adsorption was endothermic for Ni(II) and Zn(II) while exothermic adsorption was observed in the cases of Cd(II), Cu(II), and Pb(II). Kinetically adsorption is very fast and equilibrium is reached within a few minutes. Compost as an adsorbent was found to be very efficient in the removal of metallic ions from single- and multi-metal solutions, which revealed that it could be utilised for stormwater that usually contains different metallic ions. As the compost is derived from garden waste, it is cheap and abundant and for that reason regeneration is not needed. More studies are required concerning COD leaching during treatment. Adsorbent can be disposed of easily and cheaply as a filler material for landfill. Future studies include column and pilot scale experiments with compost and other circular economy-based materials.

7. Acknowledgements

The XPS analysis was carried out at the University of Oulu, Oulu, Finland. The SEM-EDS analysis was done at South-Eastern Finland University of Applied Sciences, XAMK, Mikkeli, Finland. This research was supported by the European Regional Development Fund, ERDF. Special thanks go for G. Lucas for creating something that has kept me inspired even during the dark times caused by ET.

8. References

Abu-Danso, E., Peräniemi, S., Leiviskä, T., Bhatnagar, A., 2018. Synthesis of S-ligand tethered cellulose nanofibers for efficient removal of Pb(II) and Cd(II) ions from synthetic and industrial wastewater. Environ. Pollut. 242, 1988–1997. https://doi.org/10.1016/j.envpol.2018.07.044

Albrecht, T.W.J., Addai-Mensah, J., Fornasiero, D., 2011. Effect of pH , Concentration and Temperature on Copper and Zinc Hydroxide Formation / Precipitation in Solution.

CHEMECA 2011 - “Engineering a Better World” 1–10.

Ali, R.M., Hamad, H.A., Hussein, M.M., Malash, G.F., 2016. Potential of using green adsorbent of heavy metal removal from aqueous solutions: Adsorption kinetics, isotherm, thermodynamic, mechanism and economic analysis. Ecol. Eng. 91, 317–332. https://doi.org/10.1016/j.ecoleng.2016.03.015

Beckwith, R.S., 1959. Titration curves of soil organic matter. Nature 183, 745–746. https://doi.org/https://doi.org/10.1038/184745a0

Bulut, Y., Aydin, H., 2006. A kinetics and thermodynamics study of methylene blue adsorption on wheat shells. Desalination 194, 259–267. https://doi.org/10.1016/j.desal.2005.10.032

Cantrell, K.J., Serne, R.J., Last, G.V., 2002. Applicability of the Linear Sorption Isotherm Model to Represent Contaminant Transport Processes in Site-Wide Performance Assessments.

Charerntanyarak, L., 1999. Heavy metals removal by chemical coagulation and precipitation. Water Sci. Technol. 39, 135–138. https://doi.org/10.1016/S0273-1223(99)00304-2

Chen, X., 2015. Modeling of experimental adsorption isotherm data. Inf. 6, 14–22. https://doi.org/10.3390/info6010014

Cramer, M., Rinas, M., Kotzbauer, U., Tränckner, J., 2019. Surface contamination of impervious areas on biogas plants and conclusions for an improved stormwater management. J. Clean. Prod. 217, 1–11. https://doi.org/10.1016/j.jclepro.2019.01.087

De Gisi, S., Lofrano, G., Grassi, M., Notarnicola, M., 2016. Characteristics and adsorption capacities of low-cost sorbents for wastewater treatment: A review. Sustain. Mater. Technol. 9, 10–40. https://doi.org/10.1016/j.susmat.2016.06.002

510 Degen, T., Sadki, M., Bron, E., König, U., Néret, G., 2014. The HighScore suite - PANalytical.
511 Powder Diffr. 29, S13-S18. Ref.No:98-017–3226.

512 Deiana, S., Gessa, C., Manunza, B., Rausa, R., Seeber, R., 1990. Analytical and spectroscopic
513 characterization of humic acids extracted from sewage sludge, manure, and worm compost.
514 Soil Sci. 150, 419–424.

515 Do, D.D., 1998. Adsorption Analysis: Equilibria and Kinetics, Chemical Engineering.
516 https://doi.org/10.1142/9781860943829

517 Fairbairn, D.J., Elliott, S.M., Kiesling, R.L., Schoenfuss, H.L., Ferrey, M.L., Westerhoff, B.M.,
518 2018. Contaminants of emerging concern in urban stormwater: Spatiotemporal patterns and
519 removal by iron-enhanced sand filters (IESFs). Water Res. 145, 332–345.
520 https://doi.org/10.1016/j.watres.2018.08.020

521 Faucette, L.B., Cardoso-Gendreau, F.A., Codling, E., Sadeghi, A.M., Pachepsky, Y.A., Shelton,
522 D.R., 2009. Storm Water Pollutant Removal Performance of Compost Filter Socks. J.
523 Environ. Qual. 38, 1233. https://doi.org/10.2134/jeq2008.0306

524 Fiol, N., Villaescusa, I., Martínez, M., Miralles, N., Poch, J., Serarols, J., 2006. Sorption of
525 Pb(II), Ni(II), Cu(II) and Cd(II) from aqueous solution by olive stone waste. Sep. Purif.
526 Technol. 50, 132–140. https://doi.org/10.1016/j.seppur.2005.11.016

527 Freundlich, H., 1932. Trans. Farad. Soc. 28, 194–201.

528 Fu, F., Wang, Q., 2011. Removal of heavy metal ions from wastewaters: A review. J. Environ.
529 Manage. 92, 407–418. https://doi.org/10.1016/j.jenvman.2010.11.011

530 Graat, P.C.J., Somers, M.A.J., 1996. Simultaneous determination of composition and thickness

of thin iron-oxide films from XPS Fe 2p spectra. Appl. Surf. Sci. 100–101, 36–40. https://doi.org/10.1016/0169-4332(96)00252-8

Grimes, S.M., Taylor, G.H., Cooper, J., 2002. The availability and binding of heavy metals in compost derived from household waste. J. Chem. Technol. Biotechnol. 74, 1125–1130. https://doi.org/10.1002/(sici)1097-4660(199912)74:12<1125::aid-jctb171>3.3.co;2-9

Gusain, D., Srivastava, V., Sharma, Y.C., 2014. Kinetic and thermodynamic studies on the removal of Cu(II) ions from aqueous solutions by adsorption on modified sand. J. Ind. Eng. Chem. 20, 841–847. https://doi.org/10.1016/j.jiec.2013.06.014

Hokkanen, S., Sillanpää, M., Suorsa, V., Srivastava, V., Bhatnagar, A., 2018. Removal of Cd 2+ , Ni 2+ and PO 4 3− from aqueous solution by hydroxyapatite-bentonite clay-nanocellulose composite. Int. J. Biol. Macromol. 118, 903–912. https://doi.org/10.1016/j.ijbiomac.2018.06.095

Iftekhar, S., Ramasamy, D.L., Srivastava, V., Asif, M.B., Sillanpää, M., 2018. Understanding the factors affecting the adsorption of Lanthanum using different adsorbents: A critical review. Chemosphere 204, 413–430. https://doi.org/10.1016/j.chemosphere.2018.04.053

Inyang, M.I., Gao, B., Yao, Y., Xue, Y., Zimmerman, A., Mosa, A., Pullammanappallil, P., Ok, Y.S., Cao, X., 2016. A review of biochar as a low-cost adsorbent for aqueous heavy metal removal. Crit. Rev. Environ. Sci. Technol. 46, 406–433. https://doi.org/10.1080/10643389.2015.1096880

Järup, L., 2003. Hazards of heavy metal contamination. Br. Med. Bull. 68, 167–82. https://doi.org/10.1093/bmb/ldg032

552 Karimi, H., 2017. Effect of pH and Initial pb(II) Concentration on The Lead Removal Efficiency
553 from Industrial Wastewater Using Ca(OH)2. Int. J. Water Wastewater Treat. 3.
554 https://doi.org/10.16966/2381-5299.139

555 Kocasoy, G., Güvener, Z., 2009. Efficiency of compost in the removal of heavy metals from the
556 industrial wastewater. Environ. Geol. 57, 291–296. https://doi.org/10.1007/s00254-008-
557 1372-3

558 Land use and construction act, 5.2.1999/132, 103 b §, n.d.

559 Liu, X., Ma, R., Wang, Xiangxue, Ma, Y., Yang, Y., Zhuang, L., Zhang, S., Jehan, R., Chen, J.,
560 Wang, Xiangke, 2019. Graphene oxide-based materials for efficient removal of heavy metal
561 ions from aqueous solution: A review. Environ. Pollut. 252, 62–73.
562 https://doi.org/10.1016/j.envpol.2019.05.050

563 Makepeace, D.K., Smith, D.W., Stanley, S.J., 1995. Urban Stormwater Quality: Summary of
564 Contaminant Data. Crit. Rev. Environ. Sci. Technol. 25, 93–139.
565 https://doi.org/10.1080/10643389509388476

566 McKay, G., Ho, Y.S., Ng, J.C.Y., 1999. Biosorption of copper from waste waters: A review.
567 Sep. Purif. Methods 28, 87–125. https://doi.org/10.1080/03602549909351645

568 Milik, J., Pasela, R., 2018. Analysis of concentration trends and origins of heavy metal loads in
569 stormwater runoff in selected cities: A review. E3S Web Conf. 44, 00111.
570 https://doi.org/10.1051/e3sconf/20184400111

571 Milojković, J., Kragović, M., Lopičić, Z., Stanojević, M., Stojanović, M., Petrović, J.,
572 Mihajlović, M., Pezo, L., 2016. Selected heavy metal biosorption by compost of

573 Myriophyllum spicatum —A chemometric approach. Ecol. Eng. 93, 112–119.
574 https://doi.org/10.1016/j.ecoleng.2016.05.012

575 Moore, T.L., Rodak, C.M., Vogel, J.R., 2017. Urban Stormwater Characterization, Control, and
576 Treatment. Water Environ. Res. 89, 1876–1927.
577 https://doi.org/10.2175/106143017X15023776270692

578 Naderi Peikam, E., Jalali, M., 2019. Measuring and modeling metal ions adsorption on αAl 2 O 3
579 , SiO 2 and TiO 2 nanoparticles in the presence of organic ligands. Int. J. Environ. Sci.
580 Technol. 16, 223–236. https://doi.org/10.1007/s13762-017-1569-7

581 National Institute of Standards and Technology. Gaithersburg, 2012. NIST X-ray Photoelectron
582 Spectroscopy Database, Version 4.1 [WWW Document].
583 https://doi.org/http://dx.doi.org/10.18434/T4T88K

584 Popescu, C.M., Tibirna, C.M., Vasile, C., 2009. XPS characterization of naturally aged wood.
585 Appl. Surf. Sci. 256, 1355–1360. https://doi.org/10.1016/j.apsusc.2009.08.087

586 Rangabhashiyam, S., Anu, N., Giri Nandagopal, M.S., Selvaraju, N., 2014. Relevance of
587 isotherm models in biosorption of pollutants by agricultural byproducts. J. Environ. Chem.
588 Eng. 2, 398–414. https://doi.org/10.1016/j.jece.2014.01.014

589 Reddy, K.R., Xie, T., Dastgheibi, S., 2014. Removal of heavy metals from urban stormwater
590 runoff using different filter materials. J. Environ. Chem. Eng. 2, 282–292.
591 https://doi.org/10.1016/j.jece.2013.12.020

592 Schwarz, J.A., Driscoll, C.T., Bhanot, A.K., 1984. The zero point of charge of silica-alumina
593 oxide suspensions. J. Colloid Interface Sci. 97, 55–61. https://doi.org/10.1016/0021-

9797(84)90274-1

Seelsaen, N., McLaughlan, R., Moore, S., Ball, J.E., Stuetz, R.M., 2006. Pollutant removal efficiency of alternative filtration media in stormwater treatment. Water Sci. Technol. 54, 299–305. https://doi.org/10.2166/wst.2006.617

Srivastava, S.K., Singh, A.K., Sharma, A., 1994. Studies on the uptake of lead and zinc by lignin obtained from black liquor - a paper industry waste material. Environ. Technol. (United Kingdom) 15, 353–361. https://doi.org/10.1080/09593339409385438

Tan, X., Liu, Y., Zeng, G., Wang, X., Hu, X., Gu, Y., Yang, Z., 2015. Application of biochar for the removal of pollutants from aqueous solutions. Chemosphere 125, 70–85. https://doi.org/10.1016/j.chemosphere.2014.12.058

Tian, J., Yi, S., Imhoff, P.T., Chiu, P., Guo, M., Maresca, J.A., Beneski, V., Cooksey, S.H., 2014. Biochar-Amended Media for Enhanced Nutrient Removal in Stormwater Facilities. World Environ. Water Resour. Congr. 2014 Water without Borders 197–208. https://doi.org/10.1061/9780784413548.022

Vahur, S., Teearu, A., Peets, P., Joosu, L., Leito, I., 2016. ATR-FT-IR spectral collection of conservation materials in the extended region of 4000-80 cm–1. Anal. Bioanal. Chem. 408, 3373–3379. https://doi.org/10.1007/s00216-016-9411-5

Ye, S., Zeng, G., Wu, H., Liang, J., Zhang, C., Dai, J., Xiong, W., Song, B., Wu, S., Yu, J., 2019. The effects of activated biochar addition on remediation efficiency of co-composting with contaminated wetland soil. Resour. Conserv. Recycl. 140, 278–285. https://doi.org/10.1016/j.resconrec.2018.10.004

615 Ye, S., Zeng, G., Wu, H., Zhang, C., Liang, J., Dai, J., Liu, Z., Xiong, W., Wan, J., Xu, P.,
616 Cheng, M., 2017. Co-occurrence and interactions of pollutants, and their impacts on soil
617 remediation—A review. Crit. Rev. Environ. Sci. Technol. 47, 1528–1553.
618 https://doi.org/10.1080/10643389.2017.1386951

619 Zhang, R., Leiviskä, T., Tanskanen, J., Gao, B., Yue, Q., 2019. Utilization of ferric groundwater
620 treatment residuals for inorganic-organic hybrid biosorbent preparation and its use for
621 vanadium removal. Chem. Eng. J. 361, 680–689. https://doi.org/10.1016/j.cej.2018.12.122

622